

research article

Genetic factors affecting intraoperative 5-aminolevulinic acid-induced fluorescence of diffuse gliomas

Kiyotaka Saito¹, Toshinori Hirai², Hideo Takeshima¹, Yoshihito Kadota², Shinji Yamashita¹, Asya Ivanova¹, Kiyotaka Yokogami¹

¹ Department of Neurosurgery, Division of Clinical Neuroscience, Faculty of Medicine, University of Miyazaki, Japan

² Department of Radiology, Division of Pathophysiological Diagnosis and Therapy, Faculty of Medicine, University of Miyazaki, Japan

Radiol Oncol 2017; 51(2): 142-150.

Received 15 December 2016

Accepted 13 March 2017

Correspondence to: Kiyotaka Saito, M.D., Department of Neurosurgery, Division of Neuroscience, Faculty of Medicine, University of Miyazaki, 5200 Kihara, Kiyotake, Miyazaki, 889-1692, Japan. Phone: +81-985-85-3128; Fax: +81-985-84-4571; E-mail: kiyotaka_saitou@med.miyazaki-u.ac.jp

Disclosure: No potential conflicts of interest were disclosed

This study was supported by a Grant-in-Aid for Clinical Research from Miyazaki University Hospital.

Background. In patients operated for malignant glioma, 5-aminolevulinic acid (5-ALA)-induced fluorescence guidance is useful. However, we occasionally experience instances of non-visible fluorescence despite a histopathological diagnosis of high-grade glioma. We sought to identify factors that influence the intraoperative visualization of gliomas by their 5-ALA-induced fluorescence.

Patients and methods. We reviewed data from 60 patients with astrocytic or oligodendroglial tumors who underwent tumor removal under 5-ALA-induced fluorescence guidance between January 2014 and December 2015. Their characteristics, preoperative magnetic resonance imaging (MRI) findings, histological diagnosis, and genetic profile were analyzed and univariate and multivariate statistical analyses were performed.

Results. In 42 patients (70%) we intraoperatively observed tumor 5-ALA fluorescence. They were 2 of 8 (25%) patients with World Health Organization (WHO) grade II, 9 of 17 (53%) with grade III, and 31 of 35 (89%) patients with grade IV gliomas. Univariate analysis revealed a statistically significant association between 5-ALA fluorescence and the isocitrate dehydrogenase 1 (IDH1) status, 1p19q loss of heterozygosity (LOH), the MIB-1 labeling index, and the tumor margin, -heterogeneity, and -contrast enhancement on MRI scans ($p < 0.001$, $p = 0.003$, $p = 0.007$, $p = 0.046$, $p = 0.021$, and $p = 0.002$, respectively). Multivariate analysis showed that the IDH1 status was the only independent, statistically significant factor related to 5-ALA fluorescence ($p = 0.009$).

Conclusions. This study identified the IDH1 status as the factor with the most influence on the 5-ALA fluorescence of diffuse gliomas.

Key words: glioma; 5-aminolevulinic acid (5-ALA); IDH1 mutation

Introduction

Although the standard treatment for malignant gliomas is the combination of maximal resection followed by radiation therapy and adjuvant chemotherapy (temozolomide)¹, their prognosis remains unfavorable. Maximal resection is the most important factor for improving the survival rate²⁻⁴,

patients who underwent complete resection benefited more from temozolomide than did patients treated by incomplete resection.⁵

According to the 2016 WHO classification, the genetic profile, *e.g.* the isocitrate dehydrogenase 1 (IDH1) mutation status and 1p19q co-deletion, is the key factor for the diagnosis and treatment of diffuse gliomas. The IDH1 mutation status is more

prognostic for overall survival than are standard histological criteria that differentiate high-grade astrocytomas.^{6,7} Also, the prognosis of IDH1 mutant glioblastoma is considerably better than of IDH1 wild-type anaplastic astrocytoma and glioblastoma^{6,7}, and methylation of the O-6-methylguanine DNA methyltransferase (MGMT) promoter in diffuse gliomas is a predictive epigenetic marker of the responsiveness to alkylating agents such as temozolomide.⁸

A naturally occurring intermediary in the heme synthetic pathway, 5-aminolevulinic acid (5-ALA)⁹, is used for the intraoperative visualization of malignant gliomas. After its administration as a pro-drug, it is metabolized at the tissue level to the active compound, protoporphyrin IX (PPIX), which is responsible for *in vivo* photosensitization.⁹ 5-ALA-induced fluorescence guidance facilitates complete tumor removal and may enhance progression-free survival.^{4,10} According to previous studies^{9,11}, no visible fluorescence was reported in 100% of World Health Organization (WHO) grade I, 81% of WHO grade II, and 25% of high-grade (WHO grades III and IV) gliomas. High-grade gliomas lacking contrast enhancement on magnetic resonance imaging (MRI) scans may not display appreciable macroscopic fluorescence.¹²

In contrast, it has been reported that 5-ALA-induced fluorescence is associated with contrast enhancement on preoperative MRI scans¹³, a high-grade WHO classification¹⁴⁻¹⁶, high tumor cellularity¹⁷⁻¹⁹, an increased MIB-1 labeling index^{12,15,19}, and a high tumor burden.¹³ Factors that account for the difference in the level of fluorescence in individual tumors remain to be clearly identified.

The aim of this study was to identify the factor(s), including MRI observations and genetic factors, with the greatest influence on intraoperative 5-ALA-induced fluorescence in patients with diffuse gliomas.

Patients and methods

Patient population

The Research Ethics Committee of the Faculty of Medicine, University of Miyazaki, approved this study; prior informed consent for inclusion in the study was obtained from all patients. They underwent tumor removal at Miyazaki University Hospital during the period from January 2014 to December 2015. We collected 71 consecutive glioma patients. Our inclusion criteria were surgery under 5-ALA-induced fluorescence guidance, a

TABLE 1. Clinical characteristics of 60 patients with diffuse gliomas

Characteristics	No. of Patients (%)
Number of patients	60 (100)
Sex	
Male	35 (58.3)
Female	25 (41.7)
Age (yrs)	
Average \pm SD	60.7 \pm 15.4
Median	62.5
Range	6 - 80
Tumor grades and subtypes (WHO 2007)	
Grade II	8 (13.3)
Astrocytoma	2 (3.3)
Oligoastrocytoma	3 (5.0)
Oligodendroglioma	3 (5.0)
Grade III	17 (28.3)
Anaplastic astrocytoma	2 (3.3)
Anaplastic oligoastrocytoma	3 (5.0)
Anaplastic oligodendroglioma	12 (20.0)
Grade IV	35 (58.3)
Localization	
Frontal	22 (36.7)
Fronto-temporal	2 (3.3)
Temporal	9 (15.0)
Temporo-parietal	5 (8.3)
Temporal & insular	2 (3.3)
Parietal	4 (6.7)
Parieto-occipital	2 (3.3)
Occipital	0 (0)
Insular	4 (6.7)
Central	8 (13.3)
Cerebellar	2 (3.3)
Tumor Status	
Primary	54 (90.0)
Recurrence	6 (10.0)

preoperative MRI evaluation, and a histological diagnosis of astrocytic or oligodendroglial tumors based on the WHO 2007 classification.²⁰ Excluded were patients with WHO grade I tumors and/or needle biopsy only. In patients who had undergone surgical resection more than once during the period, data from the first resection were used. Of

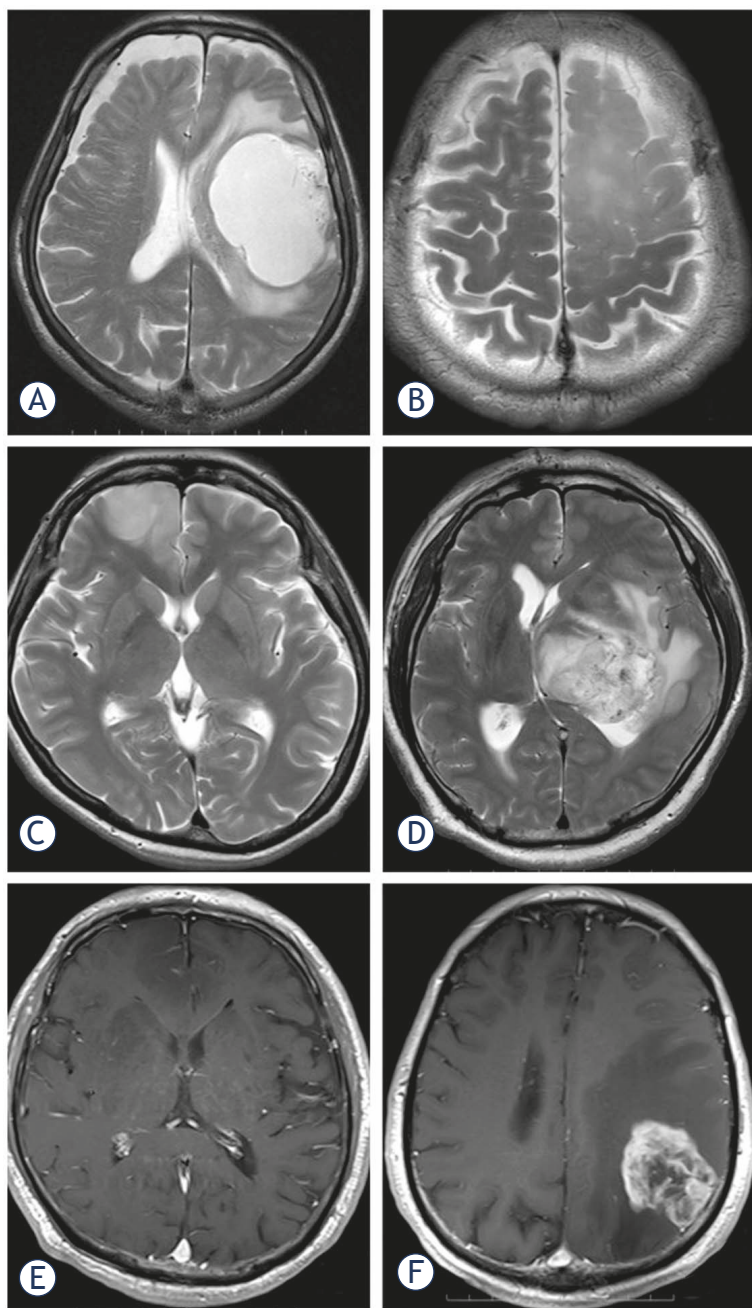


FIGURE 1. Comparison of tumor characteristics on MRI scans. Axial T2W images showing a mass with (A) a smooth and (B) an indistinct tumor border in the left frontal lobe, (C) homogeneous intensity in the right frontal lobe, and (D) heterogeneous intensity in the left thalamus. Axial gadolinium-enhanced T1W images show that (E) the tumor lacks contrast enhancement in the right frontal lobe and is (F) contrast-enhanced in the left parietal lobe.

the 71 patients, 60 (35 men, 25 women; age range 6-80 years, mean age 60.7 years) with astrocytic or oligodendroglial tumors fulfilled our selection criteria; 54 (90.0%) harbored newly diagnosed gliomas. The patient characteristics, histological diag-

nosis, and tumor location are shown in Table 1. Of the included patients, 35 (58.3%) had WHO grade IV, 17 (28.3%) WHO grade III, and 8 (13.3%) had WHO grade II gliomas. The tumor location was the frontal lobe (22 patients, 36.7%), followed by the temporal lobe (9 patients, 15.0%). In 8 patients (13.3%) the tumor was centrally located in the basal ganglion, corpus callosum, and brain stem; none of the tumors were occipital.

Preoperative MRI

All preoperative MRI studies were performed within a week before surgery on a 3 Tesla scanner (Magnetom Verio; Siemens, Erlangen, Germany). T1- and T2-weighted- (T1W, T2W), and contrast-enhanced T1W axial images were used for analysis. The images were assessed consensually by two neuroradiologists blinded to the genotype and the 5-ALA-induced fluorescence of each lesion. They used methods described elsewhere²¹ to qualitatively assess the following findings: a sharp or indistinct tumor border, homogeneous or heterogeneous signal intensity throughout the tumor on T1W and T2W images, and the presence or absence of contrast enhancement on contrast-enhanced T1W images (Figure 1). Identification of the predominant characteristics of individual tumors was based on the readers' judgment of the tumor border and signal heterogeneity.

Surgical procedure

5-ALA (20 mg/kg) was orally administered 3 hours before surgery. For the operation we used an OPMI Pentero instrument (Zeiss, Oberkochen, Germany) equipped with BLUE 400 for visualizing fluorescence and for neuro-navigation. All resections were performed with navigational guidance using contrast-enhanced axial, coronal, and sagittal T1W- or fluid-attenuated inversion recovery (FLAIR) images. The targets for tissue sampling were selected by choosing contrast-enhanced lesions and neuro-navigation, or the tumor center of high-intensity lesions on FLAIR images. Fluorescence was checked repeatedly under our modified neurosurgical microscope by switching between white- and blue-violet excitation light in different areas of the lesion during each procedure. Fluorescence was categorized subjectively by two operating surgeons; a 3rd surgeon confirmed their judgment by reviewing a movie obtained intraoperatively. Fluorescence was categorized as non-visible (negative) and visible (positive).^{19,22} Positive fluorescence included mild



FIGURE 2. Appearance of the tumor cavity under the surgical microscope. (A-B) Violet-blue light excitation yielding visible 5-ALA fluorescence. Note robust (lava-like orange) (A) and mild (pink) brightness (B). (C) No 5-ALA fluorescence is visualized in the tumor cavity.

(pink) and robust brightness (lava-like orange)¹⁸ (Figure 2).

Pathological diagnosis

To diagnose the tumors histopathologically, neuropathologists used the 2007 WHO classification of central nervous system tumors.²⁰ They were blinded to intraoperative 5-ALA fluorescence. Tumor cell proliferation was assessed immunohistochemically using MIB-1 antibody (anti-Ki-67, 1:50; DAKO, Hamburg, Germany). The highest density of Ki-67 immunopositive cells was evaluated in hot spots. The percentage of immunolabeled tumor cell nuclei was expressed as the MIB-1 labeling index.

IDH1 mutation analysis

IDH1 mutation was confirmed by immunohistochemical analysis using R132H antibody²³ or by direct sequencing. Immunostaining was according to the manufacturer's protocol. Briefly, formalin-fixed paraffin-embedded tissue was sliced into 2- μ m sections and dried at 42°C for 3 hours. Deparaffinization was with xylene, rehydration was by submerging the tissue samples in graded series of ethanol (100% to 70%, decreased in 10% steps). Phosphate-buffered saline (PBS) was used for washing. For antigen retrieval, slides were pre-treated by steaming with citric acid buffer (pH 6.0) for 20 min in an autoclave. The sections were then treated with 10% H₂O₂ for 10 min at room temperature to block endogenous peroxidase activity. After washing in 3 changes of PBS for 5 min, the sections were immunostained with monoclonal anti-human IDH1-R132H antibody (1:20 dilution, H09, Dianova, Hamburg, Germany) diluted with PBS, and incubated at 4°C overnight. After being

washed in 3 changes of PBS buffer, the tissues were covered by anti-mouse specific second antibody administered in 1 - 3 drops per slide (Dako EnVision, Hamburg, Germany), and held for 30 min at room temperature. After being washed in 3 changes of PBS buffer, the staining reaction was performed by covering the tissue with a prepared 3, 3'-diaminobenzidine (DAB) chromogen solution (1 drop of DAB chromogen for every 1000 μ l of PBS). This was followed by incubation for approximately 40 sec to allow for proper brown color development. A definite cytoplasmic immunoreaction product was scored as staining cells. Staining was scored on a two-grade scale as negative (no or < 10% staining), and as positive (> 10% positively stained cells).

Direct DNA sequencing was as previously described.^{23,24} IDH1 genomic DNA was isolated from frozen tissue samples with a QIAamp DNA Mini Kit (QIAGEN, Tokyo, Japan). A spanning 90-base pair (bp) fragment was identified with the sense primer IDH1 (forward: 5'-GGCTTGTGAGTGGATGGGTA-3') and the antisense primer IDH (reverse: 5'-GCAAAATCACATTATTGCCAAC-3'). The 25- μ l reaction mixture contained 50 ng of tumor genomic DNA, 1 μ l of each forward and reverse primer (10 μ M), 12.5 μ l of GoTaq Hot Start Green Master Mix (Promega K.K., Tokyo, Japan), and an amount of deionized water to obtain a total volume of 25 μ l. Genomic DNA was subjected to polymerase chain reaction (PCR) amplification, initial denaturation at 95°C for 2 min, and 35 cycles of amplification consisting of denaturation at 95°C for 30 sec, annealing at 58°C for 30 sec, and extension at 72°C for 20 sec. Final extension was performed at 72°C for 5 min. The 100-bp PCR amplification products were confirmed by 2% agarose gel electrophoresis.

TABLE 2. 5-aminolevulinic acid-induced fluorescence (5-ALA) in 60 diffuse gliomas

5-ALA fluorescence	WHO grade II	WHO grade III	WHO grade IV
Positive	2/8 (25 %)	9/17 (53 %)	31/35 (89%)
Negative	6/8 (75 %)	8/17 (47 %)	4/35 (11%)

The sequence reactions were performed by using a Big Dye Terminator v1.1 Cycle Sequencing Kit (Thermo Fisher Scientific K.K., Yokohama, Japan) in a 20- μ l reaction mixture comprised of 1 μ l of the 100-bp PCR products, 4 μ l of PCR buffer, 2 μ l of the forward primer (5 μ M), 12 μ l of deionized water and 1 μ l of Big Dye Terminator Ready Reaction Mix. Initial denaturation was performed at 96° for 1 min and 25 cycles of amplification (denaturation at 96° for 30 sec, annealing at 50° for 5 sec, and extension at 60° for 4 min). Sequencing products were immediately submitted to direct sequencing on an ABI PRISM 310 Genetic Analyzer (Thermo Fisher Scientific K.K., Yokohama, Japan).

Fluorescence *in situ* hybridization (FISH)

FISH analysis of 1p19q loss of heterozygosity (LOH) was performed on formalin-fixed paraffin-embedded 5- μ m tissues²⁵ prepared for dual-probe hybridization with Vysis LSI FISH Probe according to the manufacturer's instructions (Abbott Japan Co. Ltd.). 1p36/1q25 and 19q13/19p13 dual-color probe sets were used for locus-specific 1p and 19q analysis, respectively, following the manufacturer's instructions (Abbott Japan). Nuclei were counterstained with 4,6-diamidino-2 phenylindole (DAPI).

Analysis of MGMT promoter methylation

Analysis of the methylation status of the MGMT promoter was performed by bisulfite modification and subsequent methylation-specific PCR assay using previously described primers.⁸ The primer sequences for the unmethylated reaction were forward: 5'-TTTGTGTTTGTATGTTTGTAGGTTTGT-3' and reverse: 5'-AACTCCACACTCTTCCAAAAA CAAACA-3'. Sequences for the methylated reaction were forward: 5'-TTTCGACGTTTCGTAGG TTTTCGC-3' and reverse: 5'-GCACTCTTCCG AAAACGAAACG-3'. The PCR conditions were 35 cycles of 30 sec each at 95°, and 60°, and 60 sec at 72°; the PCR products were electrophoresed on 15% polyacrylamide gels as previously described.²⁶

Statistical analysis

All numeric data were reported as the mean \pm standard deviation. The positive predictive value (PPV) of 5-ALA fluorescence for high-grade gliomas was calculated as the number of 5-ALA fluorescence-positive high grade gliomas / number of all 5-ALA fluorescence-positive tumors. Its negative predictive value (NPV) was calculated as the number of 5-ALA fluorescence-negative low-grade gliomas (WHO grade II) / number of all 5-ALA fluorescence-negative tumors. The diagnostic accuracy of 5-ALA fluorescence for high-grade gliomas was calculated as the number of 5-ALA fluorescence-positive high-grade gliomas plus the number of 5-ALA fluorescence-negative low grade gliomas / the number of all tumors.

Univariate and multivariate logistic regression analyses were used to identify clinical characteristics and genetic- and imaging features associated with the 5-ALA-induced fluorescence of the lesions. Univariate analysis was with the χ^2 -, the Fisher exact-, or the Student *t*-test. Variables with $p < 0.05$ by univariate analysis were used for multivariate analysis. In multivariate logistic regression analysis we computed the odds ratio (OR) and the accompanying 95% confidence interval (CI) using samples with non-visible fluorescence for reference. *P* values < 0.05 were considered statistically significant. All statistical analyses were performed with SPSS software (version 23; IBM SPSS, Chicago IL, USA).

Results

Intraoperative 5-ALA fluorescence

Among the 60 tumors, 42 (70%) were 5-ALA fluorescence-positive; the others were negative. Of the 8 WHO grade II gliomas, 2 were positive, as were 9 of 17 (53%) WHO grade III and 31 (89%) of 35 grade IV gliomas (Table 2). For high-grade gliomas, the PPV of 5-ALA fluorescence was 95.2%; the NPV was 33.3%, and diagnostic accuracy was 76.7%.

As shown in Table 3, among the 60 diffuse gliomas, 13 (22%) harbored IDH1 mutations. These were more often seen in grade II (4/8, 50%) and grade III gliomas (7/17, 41%) than in glioblastomas (2/35, 6%). Of the 13 tumors with IDH1 mutations, 2 (15%) manifested visible fluorescence, the other 11 did not.

Univariate analysis revealed a statistically significant association between 5-ALA fluorescence and the IDH1 status (mutated, non-mutated),

1p19q LOH, MIB-1, and the margin, heterogeneity, and contrast enhancement of the tumors ($p < 0.001$, $p = 0.003$, $p = 0.007$, $p = 0.046$, $p = 0.021$, and $p = 0.002$, respectively); neither the patient age nor the MGMT methylation status was significantly associated. Multivariate analysis showed that the IDH1 status was the only independent, statistically significant factor related to 5-ALA fluorescence ($p = 0.009$) (Table 4). Using tissue samples with non-visible fluorescence as the reference, we found that the OR (95% CI) for IDH1 wild type was 19.238 (1.39, 175.39). No other factors had a significant effect on 5-ALA fluorescence.

Discussion

In this study, we analyzed factors that influence the intraoperative visualization of gliomas by their 5-ALA-induced fluorescence. Our results demonstrate that the IDH1 status was the only independent, statistically significant factor related to 5-ALA fluorescence.

As in an earlier study¹⁵, significantly more high- than low-grade gliomas exhibited 5-ALA fluorescence. Others^{12,15,18,27} reported that MIB-1, an indicator of proliferation activity, and 5-ALA fluorescence were positively correlated. Widhalm *et al.*²⁷ who documented a significantly higher proliferation rate in the tumor area with- than without 5-ALA fluorescence found that visible 5-ALA fluorescence was correlated with a MIB-1 $\geq 10\%$. On the other hand, according to Lau *et al.*¹⁸ 5-ALA intensity is a strong predictor of the degree of tumor cellularity in the most highly fluorescent areas but less predictive in areas with lower 5-ALA intensities. A significant difference in the contrast enhancement of fluorescing and nonfluorescing tissue on T1W MRI scans has been reported.¹³ Our multivariate analysis showed that the IDH1 status was the only independent, significant factor affecting 5-ALA fluorescence.

Yang *et al.*²⁸ showed that in tumor cells the IDH1 mutation may lead to the accumulation of tricarboxylic acid (TCA) cycle metabolites. This results in the activation of the heme biosynthesis pathway that works to remove TCA metabolites. Inactivation of the TCA cycle by fumarate hydratase deficiency involves the biosynthesis and degradation of heme; this facilitates the use of accumulated TCA cycle metabolites and partial mitochondrial nicotinamide adenine dinucleotide (NADH) production.²⁹ A comparison of wild-type- and IDH1-mutant U87MG cell lines showed that mutated

TABLE 3. Relationship between 5-aminolevulinic acid-induced fluorescence (5-ALA) status and clinical-pathologic features

Clinical-pathologic features	Patients with visible fluorescence (n=42)	Patients with no visible fluorescence (n=18)	P value	χ^2 , Fisher, or Student t test
Age (years)				
Average \pm SD	62.4 \pm 16.4	56.7 \pm 12.5	0.16	-
IDH1 mutation			<0.001	23.57
Positive	2	11		
Negative	40	7		
1p19q LOH			0.003	10.22
Positive	5	9		
Negative	37	9		
MGMT methylation			0.05	4.35
Positive	18	13		
Negative	24	5		
MIB1 LI (%)				
Average \pm SD	38.5 \pm 20.7	20.2 \pm 22.8	0.007	-
Tumor margin			0.046	4.88
Irregular	27	6		
Smooth	15	12		
T2 Heterogeneity			0.021	6.48
Homo	2	5		
Hetero	40	13		
Contrast enhancement			0.002	11.71
Positive	41	12		
Negative	1	6		

TABLE 4. Multivariate analysis of significant factors from univariate analysis

Factor	P Value	Odds ratio	95% confidence interval
IDH1 wild type	0.009	19.238	1.39, 175.39
1p19q LOH	0.198	0.301	0.05, 1.87
MIB-1 labeling index	0.157	1.033	0.99, 1.08
Tumor margin	0.743	0.720	0.10, 5.15
T2 heterogeneity	0.470	2.763	0.18, 43.44
Contrast enhancement	0.345	4.107	0.22, 77.32

states of IDH1 are linked to enhance 5-ALA fluorescence.²⁴ Paradoxically, glioma tissue harboring IDH1 mutations accumulated high levels of 2-hydroxyglutarate (2HG) while the level of other TCA cycle metabolites, including alpha-ketoglutarate, malate, fumarate, succinate, and isocitrate, was not significantly altered.³⁰ These observations suggest

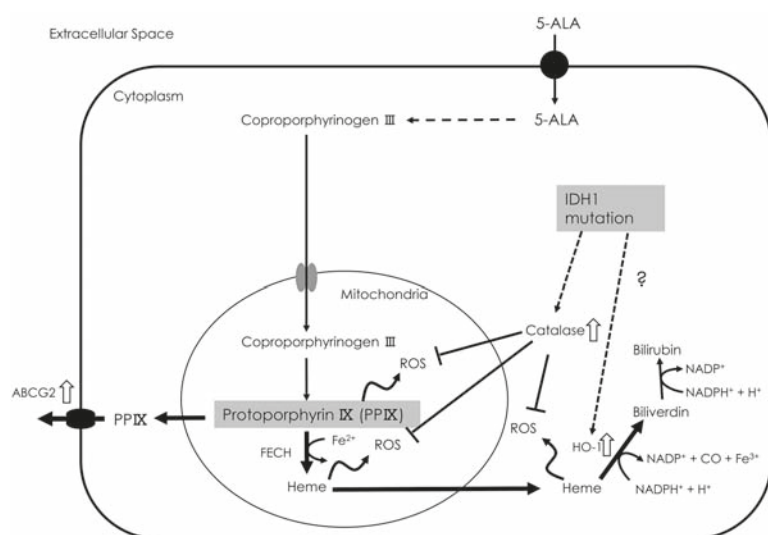


FIGURE 3. Schematic illustration of the relationship between heme synthesis and the IDH1 mutation. Thick arrows indicate metabolism activation, white arrows the activated enzymes or plasma membrane structures involved in porphyrin metabolism. ABCG2 transports porphyrins from the cytoplasm to the extracellular space. NADP⁺ levels increase during metabolization to bilirubin by heme. The IDH1 mutation may promote a defense system against ROS by activating catalase, HO-1, etc. The intracellular PPIX level is downregulated. (ABCG2 = ATP-binding cassette transporter G2; CO = carbon monoxide; FECH = ferrochelatase; HO-1 = heme oxygenase-1; PP = protoporphyrin; ROS = reactive oxygen species).

that IDH1 mutant gliomas do not involve the activation of heme biosynthesis via activation of the TCA cycle.

The increased production of reactive oxygen species (ROS) was suggested to be implicated in human glioma tumorigenesis.³¹ However, in embryonic brain cells from IDH1-mutant mice, intracellular ROS levels were dramatically reduced and the NADP⁺/NADPH ratio and catalase activity were increased.³² We hypothesize that the acquisition of IDH1 mutations by low-grade gliomas upgrades their cell protection from oxidative injury. For example, heme oxygenase-1 (HO-1), one of the most important molecules affording protection against oxidative stress³³, is a microsomal and mitochondrial enzyme.³⁴ HO-1 catalyzes the oxidation of heme to biologically harmless products, *i.e.* carbon monoxide (CO), biliverdin (rapidly reduced to bilirubin), and ferrous iron. The treatment of melanoma cells with ALA during photodynamic therapy increased the accumulation of PPIX and concomitantly enhanced HO-1 expression.³⁵ Hagiya *et al.*³⁶ reported that the messenger RNA level of HO-1 and of ATP-binding cassette transporter G2 (ABCG2), a transporter of porphyrins from the cytoplasm to the extracellular space

across the plasma membrane, was markedly increased when HepG2 cells were exposed to PPIX and visible light. These observations lead us to suspect that the difficulty in inducing fluorescence in IDH1-mutated gliomas is attributable to the establishment of a defense system against oxidative stress (Figure 3).

Although our study population was small, 22% of our 60 patients manifested IDH1 mutations. As in earlier studies^{7,37,38}, the incidence of the IDH1 mutation was highest in patients with WHO grade II gliomas. While there might be a difference in the frequency of IDH1 mutations between the Japanese and other populations, of our 8 WHO grade II gliomas, 75% were 5-ALA fluorescence-negative, a finding similar to that reported by others.^{11,19} Interestingly, in both patients with 5-ALA fluorescence-positive grade II gliomas, IDH1 was wild-type. One of the patients died as a result of malignant transformation 24 months after the operation. Ballester *et al.*³⁹ L. Y. </author><author>Olar, A. </author><author>Roy-Chowdhuri, S. </author></authors></contributors><auth-address>Department of Pathology and Genomic Medicine, Houston Methodist Hospital, Houston, Texas (L.Y.B. proposed that IDH1/2 wild-type gliomas be classified as molecular glioblastomas because, although the pathological diagnosis is low-grade glioma, the prognosis of patients with IDH1/2 wild-type gliomas is unfavorable. They also stated that the molecular subclassification of brain tumors identified important glioma subgroups whose prognosis is favorable and that mutations in IDH1/2, TP53, ATRX, and a 1p19q co-deletion suffice for the accurate molecular classification of diffuse gliomas. Even when the intraoperative pathological diagnosis is low-grade glioma, 5-ALA fluorescence positivity alerts to biological malignancy.¹⁴

The PPV value of fluorescence as an indicator of high-grade gliomas was very high although the NPV was only 33%. Therefore, the possibility of high-grade glioma in the absence of intraoperative 5-ALA fluorescence cannot be excluded.

The IDH1 mutation status of diffuse gliomas is important as the mutation played a strong role in the intraoperative absence of 5-ALA fluorescence. The ability to identify the IDH1 status intraoperatively based on the presence or absence of fluorescence of tumor tissue may be useful for determining the appropriate degree of resection.

Our study has some limitations. First, as our study population was relatively small, our findings warrant validation studies in larger cohorts. Second, fluorescence was evaluated qualitatively

and subjectively by experienced surgeons and quantitative assessment may yield more objective results.

Conclusions

Our study identified the IDH1 status as the only independent, statistically significant factor related to 5-ALA fluorescence. Further studies in a large population are required to clarify the association between the genetic status and the intraoperative 5-ALA-induced fluorescence of diffuse gliomas.

Acknowledgments

We thank Ayumi Nagatomo for technical assistance.

References

- Stupp R, Mason WP, van den Bent MJ, Weller M, Fisher B, Taphoorn MJ, et al. Radiotherapy plus concomitant and adjuvant temozolomide for glioblastoma. *N Engl J Med* 2005; **352**: 987-96. doi: 10.1056/NEJMoa043330
- Lacroix M, Abi-Said D, Fourney DR, Gokaslan ZL, Shi W, DeMonte F, et al. A multivariate analysis of 416 patients with glioblastoma multiforme: prognosis, extent of resection, and survival. *J Neurosurg* 2001; **95**: 190-8. doi: 10.3171/jns.2001.95.2.0190
- Sanai N, Polley MY, McDermott MW, Parsa AT, Berger MS. An extent of resection threshold for newly diagnosed glioblastomas. *J Neurosurg* 2011; **115**: 3-8. doi: 10.3171/2011.2.JNS10998
- Stummer W, van den Bent MJ, Westphal M. Cytoreductive surgery of glioblastoma as the key to successful adjuvant therapies: new arguments in an old discussion. *Acta Neurochir (Wien)* 2011; **153**: 1211-8. doi: 10.1007/s00701-011-1001-x
- Almenawer SA, Badhiwala JH, Alhazzani W, Greenspoon J, Farrokhyar F, Yarasavitch B, et al. Biopsy versus partial versus gross total resection in older patients with high-grade glioma: a systematic review and meta-analysis. *Neuro Oncol* 2015; **17**: 868-81. doi: 10.1093/neuonc/nou349
- Hartmann C, Hentschel B, Wick W, Capper D, Felsberg J, Simon M, et al. Patients with IDH1 wild type anaplastic astrocytomas exhibit worse prognosis than IDH1-mutated glioblastomas, and IDH1 mutation status accounts for the unfavorable prognostic effect of higher age: implications for classification of gliomas. *Acta Neuropathol* 2010; **120**: 707-18. doi: 10.1007/s00401-010-0781-z
- Yan H, Parsons DW, Jin G, McLendon R, Rasheed BA, Yuan W, et al. IDH1 and IDH2 mutations in gliomas. *N Engl J Med* 2009; **360**: 765-73. doi: 10.1056/NEJMoa0808710
- Esteller M, Garcia-Foncillas J, Andion E, Goodman SN, Hidalgo OF, Vanaclocha V, et al. Inactivation of the DNA-repair gene MGMT and the clinical response of gliomas to alkylating agents. *N Engl J Med* 2000; **343**: 1350-4. doi: 10.1056/NEJM200011093431901
- Regula J, MacRobert AJ, Gorchein A, Buonaccorsi GA, Thorpe SM, Spencer GM, et al. Photosensitisation and photodynamic therapy of oesophageal, duodenal, and colorectal tumours using 5 aminolevulinic acid induced protoporphyrin IX - a pilot study. *Gut* 1995; **36**: 67-75.
- Stummer W, Pichlmeier U, Meinel T, Wiestler OD, Zanella F, Reulen HJ, et al. Fluorescence-guided surgery with 5-aminolevulinic acid for resection of malignant glioma: a randomised controlled multicentre phase III trial. *Lancet Oncol* 2006; **7**: 392-401. doi: 10.1016/S1470-2045(06)70665-9
- Valdes PA, Jacobs V, Harris BT, Wilson BC, Leblond F, Paulsen KD, et al. Quantitative fluorescence using 5-aminolevulinic acid-induced protoporphyrin IX biomarker as a surgical adjunct in low-grade glioma surgery. *J Neurosurg* 2015; **123**: 771-80. doi: 10.3171/2014.12.JNS14391
- Ishihara R, Katayama Y, Watanabe T, Yoshino A, Fukushima T, Sakatani K. Quantitative spectroscopic analysis of 5-aminolevulinic acid-induced protoporphyrin IX fluorescence intensity in diffusely infiltrating astrocytomas. *Neurol Med Chir (Tokyo)* 2007; **47**: 53-7; discussion 57.
- Roberts DW, Valdes PA, Harris BT, Fontaine KM, Hartov A, Fan X, et al. Coregistered fluorescence-enhanced tumor resection of malignant glioma: relationships between delta-aminolevulinic acid-induced protoporphyrin IX fluorescence, magnetic resonance imaging enhancement, and neuropathological parameters. Clinical article. *J Neurosurg* 2011; **114**: 595-603. doi: 10.3171/2010.2.JNS091322
- Valdes PA, Kim A, Brantsch M, Niu C, Moses ZB, Tosteson TD, et al. δ -aminolevulinic acid-induced protoporphyrin IX concentration correlates with histopathologic markers of malignancy in human gliomas: the need for quantitative fluorescence-guided resection to identify regions of increasing malignancy. *Neuro Oncol* 2011; **13**: 846-56. doi: 10.1093/neuonc/nor086
- Jaber M, Wolfer J, Ewelt C, Holling M, Hasselblatt M, Niederstadt T, et al. The Value of 5-Aminolevulinic acid in low-grade gliomas and high-grade gliomas lacking glioblastoma imaging features: an analysis based on fluorescence, magnetic resonance imaging, 18F-fluoroethyl tyrosine positron emission tomography, and tumor molecular factors. *Neurosurgery* 2016; **78**: 401-11; discussion 411. doi: 10.1227/NEU.0000000000001020
- Johansson A, Palte G, Schnell O, Tonn JC, Herms J, Stepp H. 5-Aminolevulinic acid-induced protoporphyrin IX levels in tissue of human malignant brain tumors. *Photochem Photobiol* 2010; **86**: 1373-8. doi: 10.1111/j.1751-1097.2010.00799.x
- Arita H, Kinoshita M, Kagawa N, Fujimoto Y, Kishima H, Hashimoto N, et al. (1)(1)C-methionine uptake and intraoperative 5-aminolevulinic acid-induced fluorescence as separate index markers of cell density in glioma: a stereotactic image-histological analysis. *Cancer* 2012; **118**: 1619-27. doi: 10.1002/cncr.26445
- Lau D, Hervey-Jumper SL, Chang S, Molinaro AM, McDermott MW, Phillips JJ, et al. A prospective Phase II clinical trial of 5-aminolevulinic acid to assess the correlation of intraoperative fluorescence intensity and degree of histologic cellularity during resection of high-grade gliomas. *J Neurosurg* 2016; **124**: 1300-9. doi: 10.3171/2015.5.JNS1577
- Widhalm G, Kiesel B, Woehrer A, Traub-Weidinger T, Preusser M, Marosi C, et al. 5-Aminolevulinic acid induced fluorescence is a powerful intraoperative marker for precise histopathological grading of gliomas with non-significant contrast-enhancement. *PLoS One* 2013; **8**: e76988. doi: 10.1371/journal.pone.0076988
- Louis DN, Ohgaki H, Wiestler OD, Cavenee WK, Burger PC, Jouvet A, et al. The 2007 WHO classification of tumours of the central nervous system. *Acta Neuropathol* 2007; **114**: 97-109. doi: 10.1007/s00401-007-0243-4
- Jenkinson MD, du Plessis DG, Smith TS, Joyce KA, Warnke PC, Walker C. Histological growth patterns and genotype in oligodendroglial tumours: correlation with MRI features. *Brain* 2006; **129**: 1884-91. doi: 10.1093/brain/awl108
- Colditz MJ, Jeffree RL. Aminolevulinic acid (ALA)-protoporphyrin IX fluorescence guided tumour resection. Part 1: Clinical, radiological and pathological studies. *J Clin Neurosci* 2012; **19**: 1471-4. doi: 10.1016/j.jocn.2012.03.009
- Agarwal S, Sharma MC, Jha P, Pathak P, Suri V, Sarkar C, et al. Comparative study of IDH1 mutations in gliomas by immunohistochemistry and DNA sequencing. *Neuro Oncol* 2013; **15**: 718-26. doi: 10.1093/neuonc/not015
- Kim JE, Cho HR, Xu WJ, Kim JY, Kim SK, Kim SK, et al. Mechanism for enhanced 5-aminolevulinic acid fluorescence in isocitrate dehydrogenase 1 mutant malignant gliomas. *Oncotarget* 2015; **6**: 20266-77. doi: 10.18632/oncotarget.4060
- Lass U, Hartmann C, Capper D, Herold-Mende C, von Deimling A, Meiboom M, et al. Chromogenic in situ hybridization is a reliable alternative to fluorescence in situ hybridization for diagnostic testing of 1p and 19q loss in paraffin-embedded gliomas. *Brain Pathol* 2013; **23**: 311-8. doi: 10.1111/bpa.12003
- Araki Y, Mizoguchi M, Yoshimoto K, Shono T, Amano T, Nakamizo A, et al. Quantitative digital assessment of MGMT immunohistochemical expression in glioblastoma tissue. *Brain Tumor Pathol* 2011; **28**: 25-31. doi: 10.1007/s10014-010-0004-2

27. Widhalm G, Wolfsberger S, Minchev G, Woehrer A, Krssak M, Czech T, et al. 5-Aminolevulinic acid is a promising marker for detection of anaplastic foci in diffusely infiltrating gliomas with nonsignificant contrast enhancement. *Cancer* 2010; **116**: 1545-52. doi: 10.1002/cncr.24903
28. Yang X, Palasuberniam P, Kraus D, Chen B. Aminolevulinic acid-based tumor detection and therapy: molecular mechanisms and strategies for enhancement. *Int J Mol Sci* 2015; **16**: 25865-80. doi: 10.3390/ijms161025865
29. Frezza C, Zheng L, Folger O, Rajagopalan KN, MacKenzie ED, Jerby L, et al. Haem oxygenase is synthetically lethal with the tumour suppressor fumarate hydratase. *Nature* 2011; **477**: 225-8. doi: 10.1038/nature10363
30. Dang L, White DW, Gross S, Bennett BD, Bittinger MA, Driggers EM, et al. Cancer-associated IDH1 mutations produce 2-hydroxyglutarate. *Nature* 2009; **462**: 739-44. doi: 10.1038/nature08617
31. Yu MO, Song NH, Park KJ, Park DH, Kim SH, Chae YS, et al. Romo1 is associated with ROS production and cellular growth in human gliomas. *J Neurooncol* 2015; **121**: 73-81. doi: 10.1007/s11060-014-1608-x
32. Sasaki M, Knobbe CB, Itsumi M, Elia AJ, Harris IS, Chio, IL, et al. D-2-hydroxyglutarate produced by mutant IDH1 perturbs collagen maturation and basement membrane function. *Genes Dev* 2012; **26**: 2038-49. doi: 10.1101/gad.198200.112
33. Liu Y, Liang Y, Zheng T, Yang G, Zhang X, Sun Z, et al. Inhibition of heme oxygenase-1 enhances anti-cancer effects of arsenic trioxide on glioma cells. *J Neurooncol* 2011; **104**: 449-58. doi: 10.1007/s11060-010-0513-1
34. Belcher JD, Beckman JD, Balla G, Balla J, Vercellotti G. Heme degradation and vascular injury. *Antioxid Redox Signal* 2010; **12**: 233-48. doi: 10.1089/ars.2009.2822
35. Na HK, Surh YJ. Oncogenic potential of Nrf2 and its principal target protein heme oxygenase-1. *Free Radic Biol Med* 2014; **67**: 353-65. doi: 10.1016/j.freeradbiomed.2013.10.819
36. Hagiya Y, Adachi T, Ogura S, An R, Tamura A, Nakagawa H, et al. Nrf2-dependent induction of human ABC transporter ABCG2 and heme oxygenase-1 in HepG2 cells by photoactivation of porphyrins: biochemical implications for cancer cell response to photodynamic therapy. *J Exp Ther Oncol* 2008; **7**: 153-67.
37. Mukasa A, Takayanagi S, Saito K, Shibahara J, Tabei Y, Furuya K, et al. Significance of IDH mutations varies with tumor histology, grade, and genetics in Japanese glioma patients. *Cancer Sci* 2012; **103**: 587-92. doi: 10.1111/j.1349-7006.2011.02175.x
38. Wang HY, Tang K, Liang TY, Zhang WZ, Li JY, Wang W, et al. The comparison of clinical and biological characteristics between IDH1 and IDH2 mutations in gliomas. *J Exp Clin Cancer Res* 2016; **35**: 86. doi: 10.1186/s13046-016-0362-7
39. Ballester LY, Olar A, Roy-Chowdhuri S. Next-generation sequencing of central nervous systems tumors: the future of personalized patient management. *Neuro Oncol* 2016; **18**: 308-10. doi: 10.1093/neuonc/nov329